Artemin Is a Vascular-Derived Neurotropic Factor for Developing Sympathetic Neurons

Yutaka Honma,[1] Toshiyuki Araki,[1] Scott Gianino,[2,3]
Allen Bruce,[1] Robert O. Heuckeroth,[2,3]
Eugene M. Johnson, Jr.,[3] and Jeffrey Milbrandt[1,4]
[1]Departments of Pathology and Internal Medicine
[2]Department of Pediatrics
[3]Department of Molecular Biology and
　Pharmacology
Washington University School of Medicine
660 South Euclid Avenue
P.O. Box 8118
St. Louis, Missouri 63110

Summary

Artemin (ARTN) is a member of the GDNF family of ligands and signals through the Ret/GFRα3 receptor complex. Characterization of ARTN- and GFRα3-deficient mice revealed similar abnormalities in the migration and axonal projection pattern of the entire sympathetic nervous system. This resulted in abnormal innervation of target tissues and consequent cell death due to deficiencies of target-derived neurotrophic support. ARTN is expressed along blood vessels and in cells nearby to sympathetic axonal projections. In the developing vasculature, ARTN is expressed in smooth muscle cells of the vessels, and it acts as a guidance factor that encourages sympathetic fibers to follow blood vessels as they project toward their final target tissues. The chemoattractive properties of ARTN were confirmed by the demonstration that sympathetic neuroblasts migrate and project axons toward ARTN-soaked beads implanted into mouse embryos.

Introduction

Neurotrophic factors play crucial roles in promoting the development and survival of the central and peripheral nervous systems. The sympathetic branch of the autonomic nervous system is supported by the well characterized neurotrophic factor nerve growth factor (NGF) (Snider and Wright, 1996; Bibel and Barde, 2000; Huang and Reichardt, 2001). NGF is a member of a family of proteins called the neurotrophins, which act through a family of tyrosine kinase receptors, the Trk family, and p75 (Barbacid, 1994). Numerous gain- and loss-of-function experiments have demonstrated the importance of NGF and other neurotrophins for neuronal survival and proper target innervation. For instance, mice expressing high levels of NGF in target tissues have increased sympathetic and sensory fiber (Albers et al., 1996), whereas, sensory neurons in NGF-deficient mice fail to properly innervate target tissues (Patel et al., 2000). Interestingly, neurotrophins do not appear important for initial outgrowth of sympathetic axons, as initial projections of sympathetic axons appear normal in TrkA-deficient em-

bryos (Fagan et al., 1996); instead, they influence sympathetic neurons at later stages of axonal innervation.

A second family of neurotrophic factors, the glial cell line-derived neurotrophic factor (GDNF) family ligands (GFLs), has recently been identified. The GFLs include GDNF, Neurturin (NRTN), Persephin (PSPN), and Artemin (ARTN) (Lin et al., 1993; Kotzbauer et al., 1996; Milbrandt et al., 1998; Baloh et al., 1998b). GFLs signal through a receptor complex composed of the Ret tyrosine kinase and a GFRα (GDNF family receptor α) binding subunit coreceptor. The GFRαs are a family of four glycosyl-phosphatidyl-inositol (GPI)-anchored proteins, GFRα1-4, which serve as preferential receptors for GDNF, NRTN, ARTN, and PSPN, respectively (Baloh et al., 2000). GFLs promote the growth and survival of several populations of CNS and PNS neurons in vitro. Recent genetic experiments have demonstrated that GFL-mediated Ret signaling is essential for proper development and/or maintenance of enteric, parasympathetic, sensory, motor, and sympathetic neurons (Baloh et al., 2000; Saarma and Sariola, 1999).

The development of the sympathetic nervous system involves the proper migration and differentiation of the sympathogenic neural crest cells (Goldstein and Kalcheim, 1991; Anderson et al., 1997; Christiansen et al., 2000; Garcia-Castro and Bronner-Fraser, 1999; Krull, 2001). Neural crest destined to form the sympathetic nervous system follow a ventromedial route to a position immediately adjacent to the dorsal aorta, where they coalesce to form a columnar structure (Britsch et al., 1998). Neuronal identity is established by a cascade of transcription factors, including Mash1, Phox2a, Phox2b, and dHand, that are induced by BMPs secreted by the dorsal aorta (Hirsch et al., 1998; Schneider et al., 1999). These transcription factors regulate expression of panneuronal genes as well as lineage-specific genes, such as tyrosine hydroxylase (TH) and dopamine β-hydroxylase (Guillemot et al., 1993; Pattyn et al., 1999). The sympathetic neuroblasts in the primary sympathetic chain migrate rostrally to generate the primordial superior cervical ganglion (SCG) and ventrally to form prevertebral ganglia as well as adrenal chromaffin cells (Fernholm, 1971; Rubin, 1985). The remaining columnar structure becomes the trunk sympathetic chain (LeDouarin, 1986). During this migration period, some sympathetic precursors begin to extend axonal processes, while others continue to proliferate. The continuing migration and axonal outgrowth proceeds in close contact with the vasculature. Indeed, because of the close relationship between differentiating sympathetic neurons and blood vessels, it has long been thought that cues arising from blood vessels regulate the migration and axon guidance of these cells (Kandel et al., 2000).

Initially, the sympathetic nervous system was thought to be normal in Ret-deficient mice except for the complete lack of the superior cervical ganglia (Durbec et al., 1996). However, later work with these mice showed that the SCG was present but aberrantly located and that the entire sympathetic nervous system displayed defects (Enomoto et al., 2001). Because mice deficient in both

[4]Correspondence: jeff@milbrandt.wustl.edu

GDNF and NRTN have normally located SCG (Moore et al., 1996; Pichel et al., 1996; Sanchez et al., 1996; Heuckeroth et al., 1999) and because PSPN does not act on peripheral neurons (Milbrandt et al., 1998), it is likely that ARTN is the Ret ligand crucial for proper development of the sympathetic nervous system. In this regard, mice lacking GFRα3, the preferential receptor for ARTN, were reported to have profound deficits in the SCG but no deficits in any other sympathetic ganglia (Nishino et al., 1999). In addition, ARTN enhances the survival, proliferation, and neurite outgrowth of sympathetic neurons in vitro (Baloh et al., 1998b; Andres et al., 2001; Enomoto et al., 2001), suggesting that ARTN influences multiple facets of sympathetic neuron development and function.

To examine the physiological roles of ARTN, we have generated and characterized both ARTN- and GFRα3-deficient mice. We found major disruptions in the migration and axonal projections of sympathetic neuroblasts in these mice; however, there was little apparent effect on cell survival or proliferation. We found that ARTN is expressed by vascular smooth muscle cells and that sympathetic fibers grow toward an ectopic source of ARTN in vivo, indicating that ARTN is an important guidance factor responsible for the close association of sympathetic fibers with blood vessels. Taken together, these studies have revealed that ARTN signaling through Ret:GFRα3 complexes is crucial for the proper development of the entire sympathetic nervous system.

Results

Generation of ARTN- and GFRα3-Deficient Mice
ARTN is a member of the GDNF family of ligands (GFLs) that signals preferentially through the Ret-GFRα3 receptor complex in vitro (Baloh et al., 1998b). To understand the physiologic function of ARTN and to examine its in vivo coreceptor specificity, we generated both ARTN and GFRα3 mutant mice using homologous recombination in embryonic stem cells. To help identify the cell types expressing either ARTN or GFRα3, a *lacZ* reporter gene was inserted into the first coding exon of ARTN, and the *tau-lacZ* reporter gene, which allows visualization of neuronal projections, was inserted into the first coding exon of the GFRα3 gene (Figures 1A and 1B). Homologous recombination events for both *ARTN* and *GFRα3* were identified by Southern blot analysis (Figures 1C and 1D left panel). To remove the neo resistance cassette, mice harboring either the mutant *ARTN* or *GFRα3* alleles were mated to mice expressing Cre recombinase under the β-actin promoter (Lewandoski et al., 1997). ARTN and GFRα3 heterozygotes displayed no obvious deficits, grew normally, and were fertile. The respective heterozygote mutant mice were mated to produce mice homozygous for either the mutant ARTN or GFRα3 alleles. To insure that the mutant alleles were true loss-of-function alleles, we isolated RNA from whole P0 pups homozygous for the mutant ARTN allele ($ARTN^{-/-}$) or the mutant GFRα3 allele ($GFR\alpha3^{tlacZ/tlacZ}$) and performed RT-PCR analysis. In each case, no ARTN or GFRα3 cDNA could be detected in the respective mutant mice (Figures 1C and 1D, right panel). Both the $ARTN^{-/-}$ and $GFR\alpha3^{tlacZ/tlacZ}$ mice were born at the expected fre-

quency and survived to adulthood. Both mutant mice were fertile and did not show any gross abnormalities other than ptosis.

ARTN Is Expressed near Sympathetic Precursors and Their Axonal Projections
To further define the roles of ARTN, we utilized the lacZ reporters incorporated into the mutant alleles to carefully examine the expression patterns of ARTN and GFRα3. Tissues from ARTN and GFRα3 heterozygotes of various ages were examined using X-gal staining (or anti-lacZ immunohistochemistry). We compared the staining with previous in situ hybridization data and found that the reporters accurately reflected the ARTN and GFRα3 expression patterns. Between E11.5 and E15.5, ARTN is primarily expressed in close proximity to migration routes for sympathetic neuroblasts and in areas of sympathetic neuron projections. For example, ARTN was expressed around the sympathetic chain at E11.5 and the SCG at E12.5 (Figures 2A and 2B). Later (E12.5–13.5), lacZ staining was observed along the carotid artery, the main projection pathway of the SCG, suggesting that ARTN guides axonal outgrowth from the SCG (Figure 2B). ARTN expression was also detected around blood vessels of the gastrointestinal tract at E13.5, including the superior mesenteric, celiac, and inferior mesenteric arteries (Figures 2D–2F; data not shown). Similar to the expression pattern around the SCG pathway, ARTN expression was initially detected around the proximal portion of these arteries, and expression proceeded distally at later developmental stages until it was finally detected in the blood vessels that enter the gut wall at E15.5. ARTN expression was also observed along intercostal arteries, the path followed by axons emanating from trunk sympathetic chain ganglia (Figure 2C). In addition, ARTN was detected in the sclerotomes but was not detected in the vicinity of the sensory ganglia (dorsal root ganglia [DRG], trigeminal ganglia [TG], or nodose-petrosal ganglia) or along the projection pathways of these sensory neurons (except where they follow blood vessels). Furthermore, in contrast to GDNF and NRTN, no expression of ARTN was detected in the CNS.

GFRα3 expression was monitored using lacZ immunohistochemistry to detect the *tau-lacZ* reporter inserted into the *GFRα3* locus in GFRα3^{tlacZ} heterozygotes. LacZ staining was observed throughout the entire sympathetic nervous system, including trunk sympathetic chain, prevertebral ganglia, and SCG at all embryonic stages examined (E11.5 through E15.5) and at P0 (Figures 2G–2I; data not shown). GFRα3 was also detected in sensory neurons including TG, DRG, and nodose-petrosal ganglia at these embryonic stages and at P0 (Figure 2G). In adult mice, GFRα3 expression was absent in sympathetic neurons and was expressed at low levels in a small percentage of DRG sensory neurons (data not shown). Furthermore, in agreement with a lack of ARTN expression in the CNS, we did not detect GFRα3 expression in the CNS using X-gal or lacZ immunohistochemistry. Thus, unlike signaling from other GFL-GFRαs, ARTN:GFRα3 signaling appears to occur solely in the peripheral nervous system. The expression of GFRα3 in sympathetic neuroblasts and the presence of ARTN

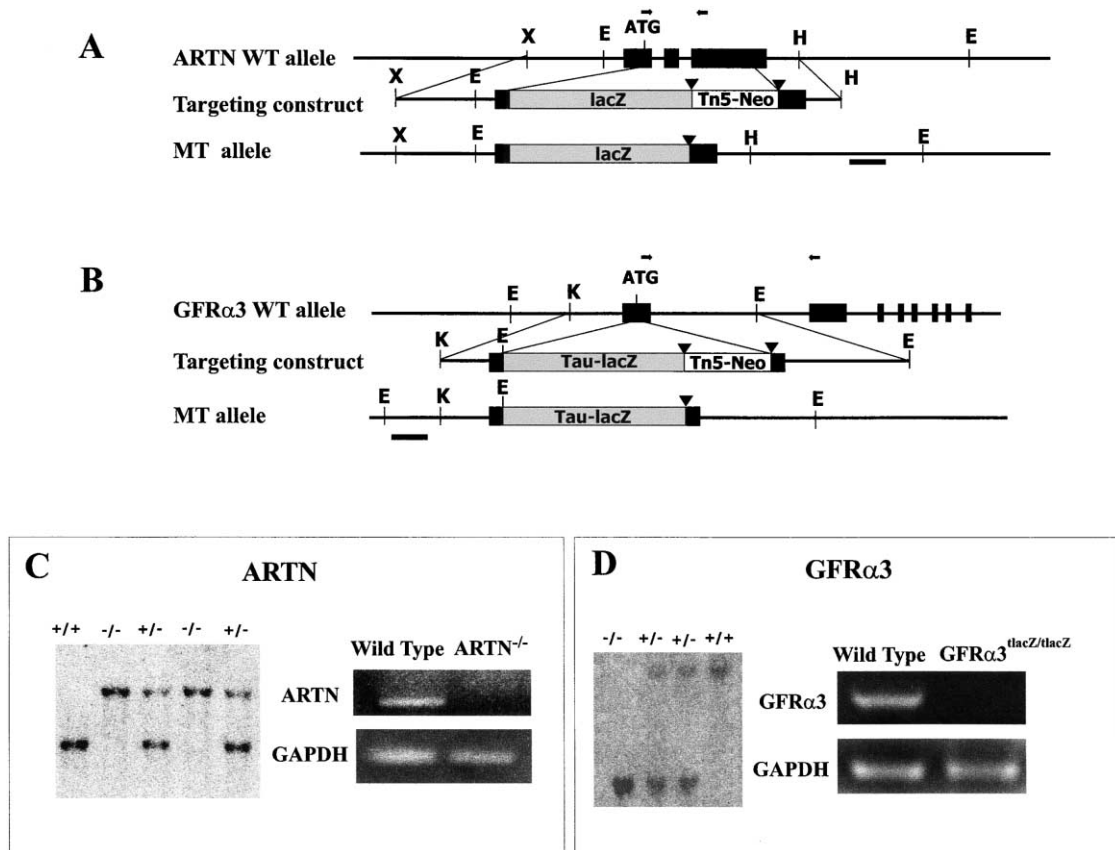Figure 1. Generation of *ARTN*^{−/−} and *GFRα3*^{tlacZ/tlacZ} Mice

The wild-type allele, targeting vector, and resulting mutant allele demonstrate the strategy used to disrupt *ARTN* (A) or *GFRα3* (B) in ES cells. Thick black bars in (A) and (B) indicate the fragment used as probe in genotyping. A loxP-flanked (black triangles) neomycin resistance cassette was used so that it could be subsequently removed using Cre recombinase. Arrows indicate the location of primers used for RT-PCR analysis in (C) and (D). Southern blot analysis of EcoRI-digested genomic DNA from F2 littermates identified ARTN ([C], left) and GFRα3 ([D], left) heterozygotes and homozygotes. RT-PCR analysis of whole P0 pups confirmed the absence of ARTN ([C], right) and GFRα3 ([D], right) mRNAs in the respective homozygous mutants. Abbreviations in (A) and (B): X, XhoI; E, EcoRI; H, HindIII; K, KpnI.

along routes of sympathetic neuroblast migration and along the path of sympathetic axonal projections suggests that ARTN might act as a guidance molecule for sympathetic neurons and their axons.

ARTN- and GFRα3-Deficient Mice Have Deficits in the Sympathetic Nervous System

In both the *ARTN*^{−/−} and *GFRα3*^{tlacZ/tlacZ} mice, approximately 30% of adult mice displayed ptosis (Figure 3). Of the mice with ptosis, 35% had bilateral ptosis, whereas 65% had unilateral ptosis with no predilection for the right or left side. Because ptosis can be caused by loss of sympathetic innervation to the superior tarsus muscle by the SCG, we examined this ganglia by preparing consecutive parasagittal sections of the adult heads from both *ARTN*^{−/−} and *GFRα3*^{tlacZ/tlacZ} mice. We found that the SCG ipsilateral to the eye displaying ptosis was either missing (30%) or small (70%) (Figure 3F) and was shifted caudally to a variable degree in affected animals (Figure 3J). The SCG in mice lacking ptosis were essentially intact, with only a minimal caudal shift in adult animals (Figure 3E). Furthermore, the SCGs that were in

the most aberrant positions were invariably associated with ptosis and were smaller than SCGs corresponding to the eye without ptosis (Figure 3F). To examine whether the abnormal SCG location in ARTN- and GFRα3-deficient mice resulted in abnormal innervation of target tissues in adulthood, TH immunohistochemistry was performed to identify the sympathetic fibers projecting to the superior tarsus muscle. Although some sympathetic fibers were detectable in a few of the affected animals (mice with ptosis), the density and distribution of the innervation was distinctly abnormal on the side with ptosis (Figure 3I) compared to wild-type animals (Figure 3G). In the mutant mice that did not display ptosis, there was no discernible defect in sympathetic innervation (Figure 3H). Indeed, in mice with unilateral ptosis, the innervation pattern from the SCG on the unaffected side was comparatively normal with respect to location and target innervation. Thus, abnormally located SCGs are smaller and fail to innervate their targets properly (shown schematically in Figure 3J).

Other regions of the sympathetic nervous system were examined using whole-mount tyrosine hydroxylase
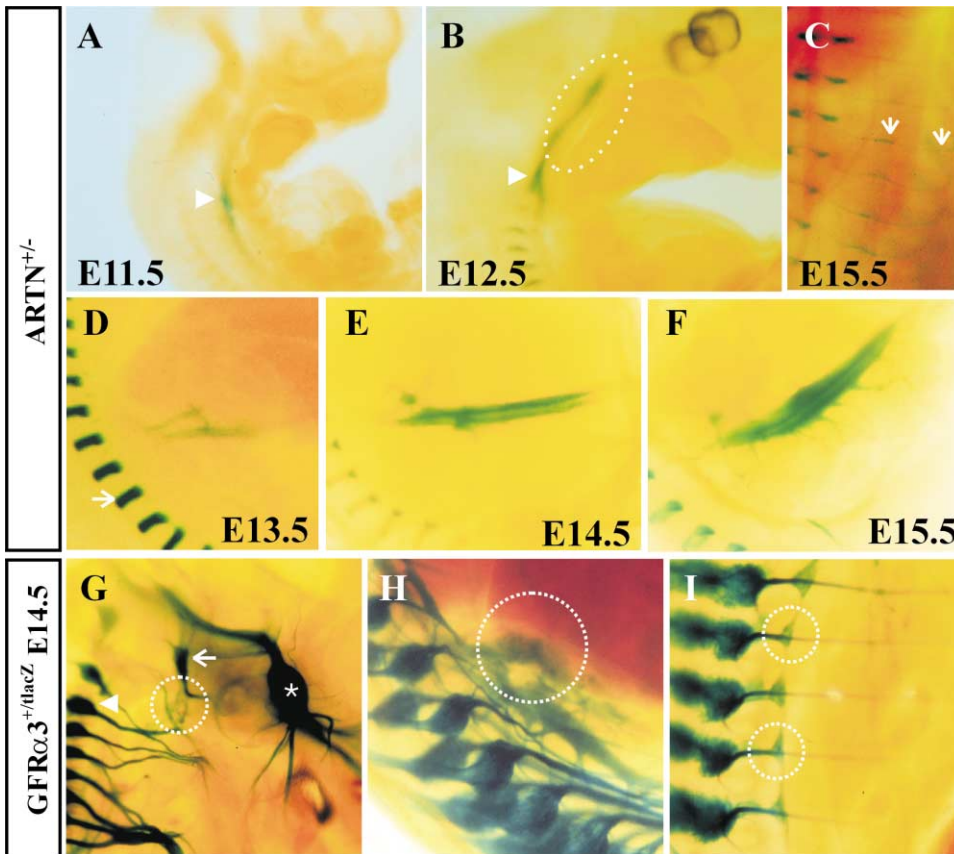
Figure 2. ARTN Is Expressed Near Sympathetic Neuroblasts and Axonal Projections

(A–F) *ARTN*^{+/−} embryos of indicated ages were stained with X-gal to demonstrate lacZ (ARTN) expression. Sagittal view of E11.5 and E12.5 revealed lacZ expression around SCG (arrowhead in [A] and [B]) and the innervation pathway of SCG (indicated by white dotted circle in [B]) at E12.5. LacZ expression was also observed around intercostal arteries at E15.5 (arrows) (C). LacZ expression was found around the superior mesenteric artery at E13.5, E14.5, and E15.5 (D–F). This expression proceeded from central to peripheral blood vessels during development (D–F). Sclerotomes (arrow) also express high levels of ARTN at E13.5.

(G–I) Sagittal view of *GFRα3*[+/tlacZ] E14.5 embryo stained with X-gal to demonstrate tau-lacZ (GFRα3) expression. SCG (white dotted circle in [G]), prevertebral ganglia (white dotted circle in [H]), and trunk sympathetic chain ganglia (white dotted circle in [I]) all express GFRα3. GFRα3 was intensely expressed in peripheral sensory ganglia (trigeminal, *; dorsal root, arrowhead; and nodose-petrosal, arrow) in (G).

(TH) immunostaining. Although the defects were not as pronounced as those found for the SCG, analysis of the adult and P0 thoracic region revealed that trunk sympathetic chain ganglia in both *ARTN*^{−/−} and *GFRα3*[tlacZ/tlacZ] mice were invariably smaller and aberrantly segmented compared to wild-type mice (Figures 4A–4C; data not shown), with the more caudal ganglia being more severely affected. These mutant mice also have abortive axonal growth, as highlighted by the failure to form fasciculated axonal bundles. These deficits were similar to those observed in Ret-deficient mice (Enomoto et al., 2001) but were not reported in a previous report characterizing *GFRα3*^{−/−} mice (Nishino et al., 1999).

The deficits in multiple sympathetic ganglia of ARTN and GFRα3 mutant mice prompted us to search for deficits in sympathetic innervation of other tissues. Because the gut is richly innervated by the sympathetic nervous system and ARTN is expressed along the major blood vessels supplying the gut, we performed whole-mount TH immunostaining of the esophagus, stomach, and

intestine. This analysis demonstrated that TH-stained fibers were present in *ARTN*^{−/−} and *GFRα3*[tlacZ/tlacZ] mice; however, the number of positive fibers was uniformly less than in wild-type mice (Figures 4D–4F). Higher magnification demonstrated that TH-positive fibers were lost from the circular muscle layer of intestine (Figures 4G–4I) as well as esophagus and stomach (data not shown). Quantitative analysis of TH-positive fibers in the circular muscle of the gut revealed major deficits in the number of fibers/grid in both *ARTN*^{−/−} and *GFRα3*[tlacZ/tlacZ] mice (mean ± SEM; wild-type, 7.4 ± 0.3; *ARTN*^{−/−}, 0.8 ± 0.1, $p < 0.00001$; *GFRα3*[tlacZ/tlacZ] 1.1 ± 0.1, $p < 0.00001$). In contrast, TH-positive fibers in the myenteric ganglia and tertiary plexus were unaffected (mean ± SEM; wild-type, 6.4 ± 0.2; *ARTN*^{−/−}, 6.3 ± 0.2, $p > 0.84$). It is unclear why there are selective deficits in these fiber populations; however, previous studies have demonstrated that the gut is innervated by distinct populations of sympathetic neurons (Costa and Furness, 1984; Schmidt et al., 1998), which may be differentially affected by ARTN deficiency. The deficits in prevertebral ganglia and gut sympathetic
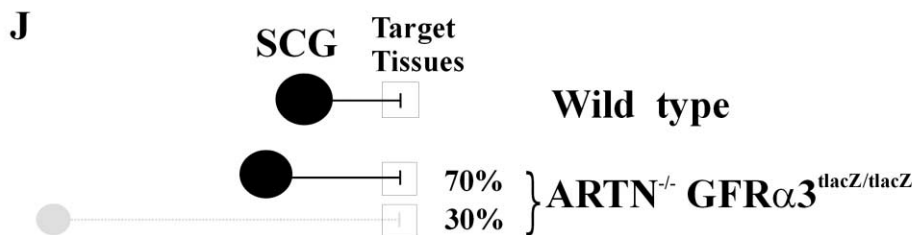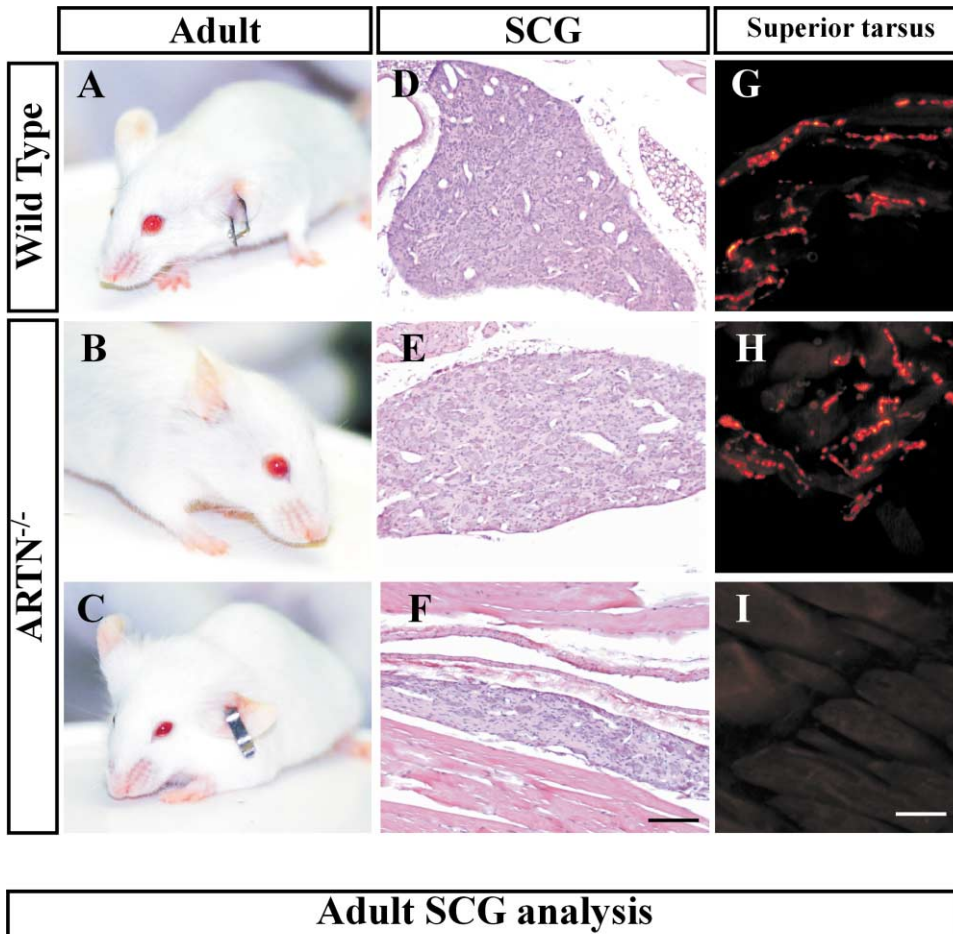
Figure 3. *ARTN*^{−/−} Mice Have Ptosis and Defects in SCG Migration and Axonal Projection

Wild-type (A) and *ARTN*^{−/−} mice (B and C). The same mouse is shown in (B) and (C) to demonstrate a unilateral defect (left side, ptosis [C]; right side, without ptosis [B]). Parasagittal sections of adult SCG demonstrate that the ganglion from the side without ptosis (E) appears morphologically identical to the wild-type SCG (D). The SCG ipsilateral to the side with ptosis is markedly reduced in size (F). The SCG innervation to the superior tarsus muscle was examined using TH-immunohistochemistry. TH-positive innervation of the non-ptosis side (H) was indistinguishable from wild-type (G), whereas TH-positive fibers did not innervate this muscle on the side with ptosis (I). A schematic representation of the SCG analysis of adult *ARTN*^{−/−} and *GFRα3*[tlacZ/tlacZ] mice (J). Parasagittal sections of adult mice (n = 20 for each genotype) were examined to determine the size and position of the SCG. This information was correlated with the eye phenotype (ptosis versus non-ptosis). Closed black circles indicate wild-type and mutant mice that did not display ptosis. A closed gray circle indicates the caudally displaced SCG in mice with ptosis. The solid line between the closed circle and open square represents the average distance between the SCG and superior tarsus muscle. The longer dotted line indicates the more caudal location of the SCG and the consequent loss of innervation in mice with ptosis. Scale bar, 100 μm in (D), (E), and (F); 50 μm in (G), (H), and (I).

innervation in *ARTN*^{−/−} and *GFRα3*[tlacZ/tlacZ] mutant mice parallel those observed in the SCG and indicate that ARTN is critical for proper sympathetic innervation in many parts of the developing mouse.

Because Ret signaling is crucial for many aspects of enteric nervous system development, we also examined the enteric nervous system in *ARTN*^{−/−} mice, but no abnormalities were detected. Specifically, neuronal size as well as neuron cell numbers were normal in the myenteric (mean number/grid ± SEM; wild-type, 59 ± 2; *ARTN*^{−/−}, 59 ± 1) and submucosal (wild-type, 50 ± 2; *ARTN*^{−/−}, 51 ± 1) ganglia of the small bowel and colon. Also, acetylcholinesterase-stained neuronal fiber density in the myenteric plexus of *ARTN*^{−/−} mice was normal.
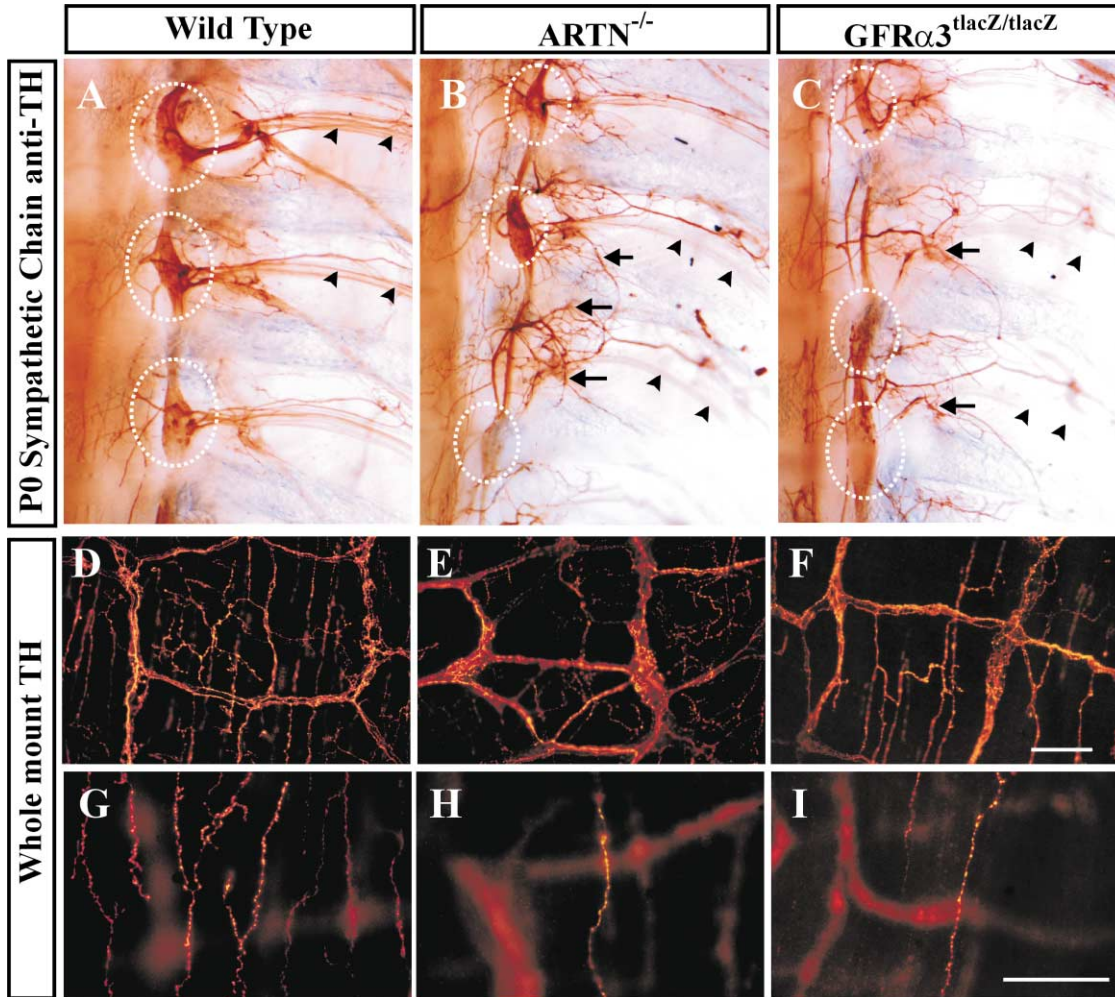
Figure 4. Trunk Sympathetic Ganglia and Sympathetic Innervation of the Gut Are Abnormal in _ARTN_$^{-/-}$ and _GFRα3_$^{tlacZ/tlacZ}$ Mice

(A–C) Whole-mount TH immunohistochemistry revealed that sympathetic chain ganglia from _ARTN_$^{-/-}$ and _GFRα3_$^{tlacZ/tlacZ}$ mice were aberrantly segmented at P0 (white dotted circle in [A]–[C] indicates each chain ganglion). Axonal bundles from each ganglion were short and misdirected in both mutants (black arrows in [B] and [C]). Sympathetic fibers to the adult gut were examined using whole-mount TH immunohistochemistry (D–I). Fewer TH-positive fibers were present in the small bowel of ARTN- and GFRα3-deficient mice compared to wild-type animals (D–F). Higher magnification revealed dramatic reductions in TH-positive fibers innervating the circular muscle layer of the small bowel in ARTN- and GFRα3-deficient mice (G–I). Scale bar, 100 μm in (D–I).

Thus, unlike GDNF and NRTN, ARTN is critical for sympathetic innervation to the gut but not for formation or maintenance of the enteric nervous system.

ARTN Does Not Directly Promote Sympathetic Neuron Survival

Previous studies of GFRα3-deficient mice found that the SCG was either missing or very small in all adult mice due to massive apoptosis of SCG neurons during postnatal development (Nishino et al., 1999). In addition, experiments using in vitro SCG cultures established from rats or mice found that ARTN can promote sympathetic neuron survival (Baloh et al., 1998b; Andres et al., 2001). These studies led to the suggestion that Ret/ GFRα3-mediated signaling via ARTN was important for promoting survival of these sympathetic neurons. The observation, however, that SCG size was normal in ARTN-deficient mice, except when the peripheral target

was not innervated, suggested the possibility that ARTN is critical for targeting sympathetic axons to their peripheral targets but not for sympathetic neuron survival in vivo. Instead, other target-derived trophic factors, such as NGF, must be critical for postnatal survival of sympathetic neurons once the axonal targets are innervated. To further investigate whether ARTN promotes SCG neuron survival postnatally in vivo, we counted SCG neurons in adult wild-type and _GFRα3_$^{tlacZ/tlacZ}$ mice. Furthermore, we compared the SCG ipsilateral to the eye with ptosis with the one corresponding to the eye without ptosis in the _GFRα3_$^{tlacZ/tlacZ}$ mice. Consistent with the gross appearance of the adult SCG (see Figure 2), there was no apparent difference in the number of SCG neurons between wild-type and _GFRα3_$^{tlacZ/tlacZ}$ if the tarsal muscle was innervated and the eye was free of ptosis (mean ± SEM; wild-type, 9703 ± 202, n = 4; mutant, non-ptosis, 10,117 ± 317, n = 3). However, the SCG
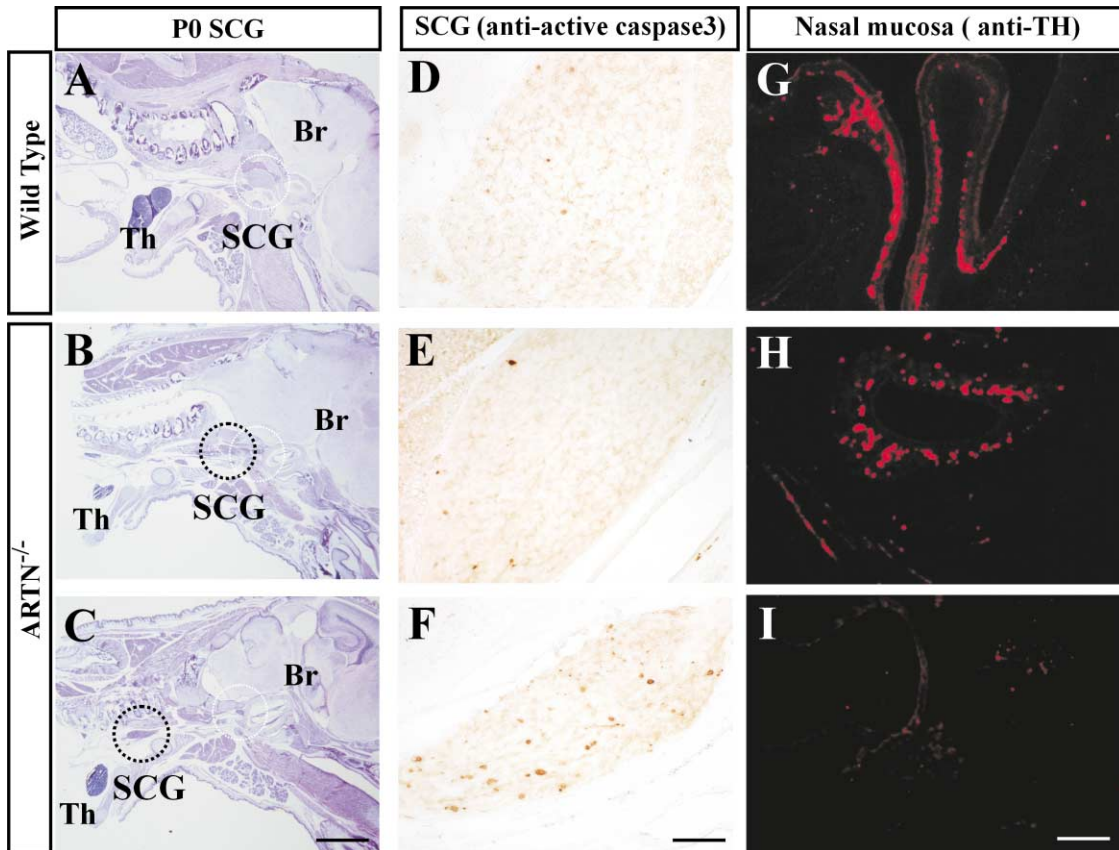
Figure 5. ARTN-Mediated Signaling Does Not Directly Influence SCG Neuronal Survival or Proliferation

Hematoxylin and eosin staining of parasagittal sections of P0 pups demonstrated that the SCG of $ARTN^{-/-}$ mice is caudally shifted to a variable degree (A–C). White dotted circles indicate wild-type SCG position. Black dotted circles indicate the position of the SCG in $ARTN^{-/-}$ mice. (D–F) Apoptotic cells in the SCG from each mouse shown in (A)–(C) were visualized by immunohistochemistry using an antibody to activated caspase-3. Significantly increased apoptosis was found in the severely shifted SCG in $ARTN^{-/-}$ mice (F). However, the mildly shifted SCG (B) did not have increased apoptosis (E) compared to wild-type animals (D). Neighboring sections from those used in (D)–(F) were stained using TH immunohistochemistry to detect sympathetic innervation (G–I). TH-positive fibers innervating the nasal mucosa from severely shifted SCG were not detected (I), whereas sympathetic innervation from mildly shifted SCG was apparently normal (H). Th, thymus; Br, brain. Scale bar, 500 μm in (A)–(C); 100 μm in (D)–(F); 50 μm in (G)–(I).

corresponding to the side with ptosis, in which innervation was defective, was smaller and contained many fewer neurons (1564 ± 853, n = 3, p < 0.009). Thus, it appears that the effect of ARTN deficiency on neuronal number is not due to a direct requirement for ARTN on neuronal survival but is rather due to an indirect effect secondary to a failure of ARTN-facilitated target innervation.

To further investigate the fate of these sympathetic neurons in the absence of ARTN, we measured cell death in the SCG at P0 using an antibody to activated caspase-3. Low levels of apoptosis were observed in the SCGs of $ARTN^{-/-}$ mice when their position was only mildly abnormal and target innervation was normal (Figures 5B, 5E, and 5H). Conversely, when the SCG was severely displaced with major deficits in target innervation, increased apoptosis of $ARTN^{-/-}$ SCG neurons was observed (Figures 5C, 5F, and 5I). These results were quantified by determining the percentage of activated caspase-3-positive cells in representative slides from the SCG of wild-type and mutant ($ARTN^{-/-}$ and $GFR\alpha3^{tlacZ/tlacZ}$) mice (n = 2). This analysis verified that

the rate of neuronal cell death in the SCG of mutant animals was normal if the SCG was only mildly shifted in position (positive cells as a percent of total neurons ± SEM was 1.9% ± 0.1% [wild-type], 1.8% ± 0.1% [mildly shifted SCG]) but was increased in severely shifted SCG (5.5% ± 0.2%, p < 0.0003). These results indicate that SCG neuronal survival is dependent on proper innervation of the target tissue rather than directly on ARTN itself. Similar studies of E12.5 and E14.5 embryonic SCG were performed to determine if ARTN promotes sympathetic neuron survival during embryogenesis, but again, no differences in the number of apoptotic cells between wild-type and mutant were observed (data not shown). Taken together, these results indicate that ARTN is not directly required for the survival of SCG neurons in utero or postnatally and that ARTN is not a direct-acting survival factor for SCG neurons in vivo. As long as proper innervation is achieved even in the absence of ARTN, neuronal survival is normal. However, if the SCG fails to innervate its targets, then there is a dramatic increase in neuronal apoptosis, presumably due to the lack of a target-derived neurotrophic factor such as NGF.
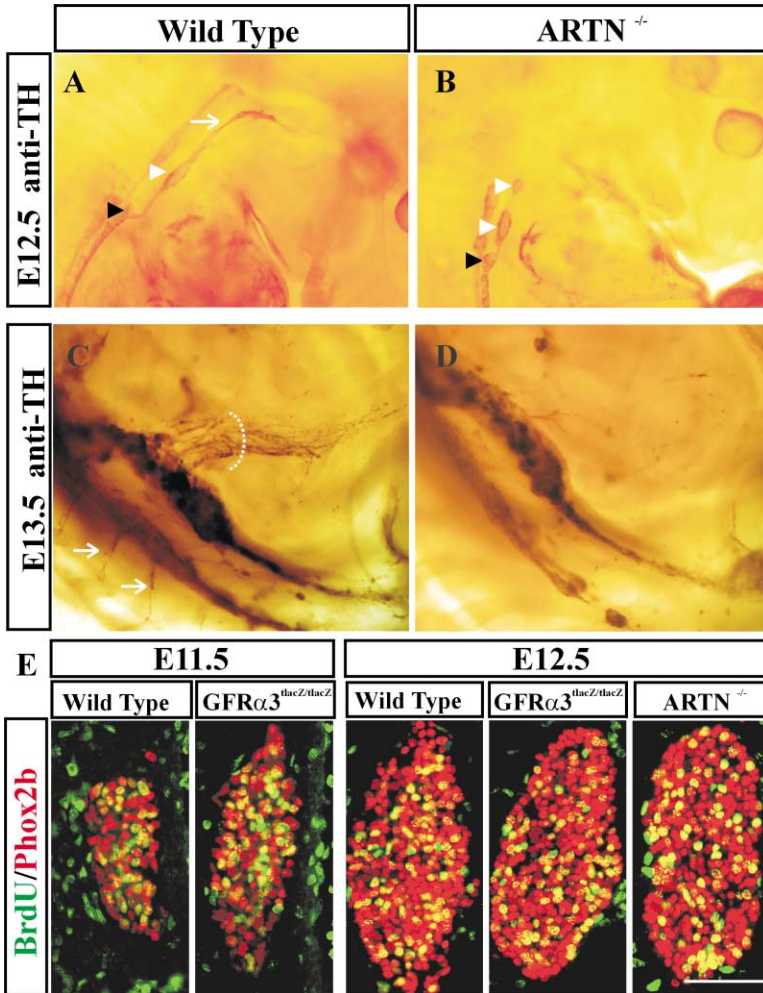
Figure 6. Sympathetic Axonal Projections Are Defective but SCG Precursor Proliferation Is Normal in $ARTN^{-/-}$ and $GFR\alpha3^{tlacZ/tlacZ}$ Embryos

Examination of sympathetic system in E12.5 and E13.5 embryos using whole-mount TH immunohistochemistry (A–D). In $ARTN^{-/-}$ mice, the SCG (white arrowheads) is located close to the stellate ganglion (STG) (black arrowhead) and is abnormally segmented. In contrast, the wild-type SCG is located more rostrally (compare the distance between STG and SCG) in wild-type versus $ARTN^{-/-}$. The wild-type SCG has a thick axon bundle emanating from it (white arrow in [A]), whereas axonal outgrowth from the mutant SCG was absent (B). At E13.5, axonal outgrowth from prevertebral ganglia was observed in wild-type (white dotted line in [C]), whereas it was severely impaired in $ARTN^{-/-}$ mice (D). Axonal outgrowth from trunk sympathetic chain (arrows) was also severely impaired in $ARTN^{-/-}$ mice (compare [C] and [D]). (E) Proliferation of SCG precursors in ARTN- and GFRα3-deficient embryos is unimpaired. Embryos of the indicated ages and genotypes were labeled with BrdU for 1 hr in utero, and proliferating SCG precursors were identified by double-label immunohistochemistry using anti-BrdU and anti-Phox2b antibodies. This analysis revealed no differences in the number of proliferating precursors between wild-type and mutant mice at any age examined. Scale bar, 50 μm in (E).

Sympathetic Deficits in ARTN-Deficient Mice Occur Early in Embryogenesis

The abnormal location of the SCG in ARTN-deficient mice suggested that migration of the sympathetic precursors may be impaired, similar to that observed in $GFR\alpha3^{-/-}$ and $Ret^{-/-}$ mice (Nishino et al., 1999; Enomoto et al., 2001). To determine whether ARTN is crucial for proper rostral migration of the SCG during development, the sympathetic nervous system in E12.5 embryos was examined using whole-mount TH immunostaining. We examined the position of the SCG in E12.5 embryos, the first stage when it is clearly demarcated. When compared to wild-type mice, the SCG in ARTN-deficient embryos is already located in a more caudal position in all cases examined (n = 30) (Figures 6A and 6B). Axonal outgrowth from the $ARTN^{-/-}$ SCG was also distinctly abnormal compared to the well formed axon bundle extending from the wild-type SCG at E12.5. Equally dramatic abnormalities in the SCG of $ARTN^{-/-}$ embryos were observed at E13.5 (data not shown). Defects were also observed in other regions of the sympathetic nervous system. For example, no sympathetic axonal outgrowth was observed along the intercostal artery (Figure 4B), and axonal outgrowth from the prevertebral ganglia was severely impaired in $ARTN^{-/-}$ mice (Figures 6C and 6D). Furthermore, the sizes of the sympathetic chain

ganglia are reduced, and the segmentation pattern is also abnormal (Figure 4B). $GFR\alpha3^{tlacZ/tlacZ}$ embryos showed similar migration and axonal projection defects as those observed in the $ARTN^{-/-}$ embryos. Thus, ARTN appears to play an important role as a guidance factor for neuronal migration and axonal growth in the entire sympathetic nervous system early in embryogenesis. The deficits in migration and axonal outgrowth were readily apparent in all mutant embryos examined, in contrast to the adults, where only a fraction of the mice had dramatically affected SCG. This indicates that ARTN exerts its primary effects as early as E12.5 and suggests that the loss of ARTN in the SCG but not in the gut is at least partly compensated for by other unidentified molecules at later stages. Taken together with previous data gleaned from studies of $GFR\alpha3^{-/-}$ and $Ret^{-/-}$ mice, these results demonstrate that ARTN-mediated signaling through Ret:GFRα3 receptor complexes is crucial for proper migration of SCG precursors during development.

The development of the sympathetic nervous system begins as neural crest cells from the neural tube migrate specifically through the rostral half of each somite to reach the dorsal aorta where they are recognized as sympathetic precursors. This distinct pattern of migration through the somites contributes to the segmental

organization of the sympathetic nervous system (Goldstein and Kalcheim, 1991). The abnormal segmentation of the trunk sympathetic chain in $ARTN^{-/-}$ and $GFR\alpha3^{tlacZ/tlacZ}$ mice suggested that ARTN-GFRα3 signaling may impact early migrating neural crest cells, even before they reach the dorsal aorta. $GFR\alpha3^{+/tlacZ}$ mice were examined using lacZ immunohistochemistry, and a few lacZ$^+$ cells were observed in the neural tube at E9.5 and E10 (data not shown). Double-label staining with lacZ and p75, to identify neural crest cells, revealed that p75$^+$ cells expressing GFRα3 had migrated into the vicinity of the dorsal aorta by E10. To determine whether lack of GFRα3 had an effect on these cells, we used Phox2b immunohistochemistry to identify sympathetic precursors surrounding the dorsal aorta at E10.5. The number of sympathetic precursors was quantified by counting the Phox2b$^+$ cells along the dorsal aorta in consecutive sections that together covered the entire forelimb area. The number of sympathetic precursors in this region was modestly decreased in the GFRα3-deficient compared to wild-type embryos (Phox2b$^+$ cells (mean $\pm$ SEM); wild-type, 46.4 $\pm$ 0.9; $GFR\alpha3^{tlacZ/tlacZ}$, 35.8 $\pm$ 2.2, p < 0.05 (n = 3 for each genotype). Thus, it appears that the lack of ARTN signaling decreases or delays the number of sympathetic neuroblasts migrating to the primordial sympathetic chain.

In addition to deficits in migration, the abnormalities observed in the SCG of $ARTN^{-/-}$ and $GFR\alpha3^{-/-}$ mice could be due to decreased cell number. We did not find evidence for increased apoptosis in the sympathetic system during embryogenesis; however, decreased proliferation could also contribute to the observed deficits. Indeed, other GFLs are important in neuroblast proliferation; in particular, GDNF is essential for proliferation of enteric and parasympathetic neuronal precursors (Chalazonitis et al., 1998; Heuckeroth et al., 1998; Hearn et al., 1998; Taraviras et al., 1999; Enomoto et al., 2000), and ARTN stimulates sympathetic neuroblast proliferation in vitro (Andres et al., 2001). To determine if ARTN affects mitogenesis, we compared the proliferation rate of sympathetic neuroblasts in wild-type and $GFR\alpha3^{tlacZ/tlacZ}$ mice. Because the abnormalities in SCG location and axonal outgrowth were apparent as early as E12.5, we determined the proliferation rate at E11.5, E12.5, and E14.5. Wild-type, $ARTN^{-/-}$, and $GFR\alpha3^{tlacZ/tlacZ}$ mice were injected with BrdU 1 hr prior to harvesting the embryos. Labeled sympathetic precursors were identified by double staining with antibodies against Phox2b and BrdU. Phox2b is a marker of early sympathetic precursors whose expression is necessary for differentiation of sympathetic neurons (Pattyn et al., 1999), and BrdU is incorporated into the nuclei of dividing cells. The number of proliferating cells appeared to be similar in wild-type, $ARTN^{-/-}$, and $GFR\alpha3^{tlacZ/tlacZ}$ mice at each of the ages examined (Figure 6E). To quantify these results, proliferating neuronal precursors were counted in representative slides from three mice of each genotype at E11.5 (mean percentage of BrdU$^+$ cells/ Phox2b$^+$ cells $\pm$ SEM; wild-type, 43.8% $\pm$ 2.4%; $GFR\alpha3^{tlacZ/tlacZ}$, 45.4% $\pm$ 3.4%), E14.5 (wild-type, 5.3% $\pm$ 0.4%; $GFR\alpha3^{tlacZ/tlacZ}$, 5.0% $\pm$ 0.2%), and E12.5 (wild-type, 32.5% $\pm$ 0.4%; $ARTN^{-/-}$, 32.1% $\pm$ 0.3%). To further examine this issue, we counted the total number of Phox2b$^+$ neuroblasts as well as the number of proliferat-

ing Phox2b$^+$ cells in the entire ganglia by examining consecutive parasagittal sections throughout the region of interest in E12.5 wild-type and $GFR\alpha3^{tlacZ/tlacZ}$ embryos (n = 3 for each). We found comparable numbers of neuroblasts (mean $\pm$ SEM; wild-type, 14,610 $\pm$ 1256; $GFR\alpha3^{tlacZ/tlacZ}$, 13,072 $\pm$ 1019; p = 0.39) and proliferating (BrdU$^+$) neuroblasts (wild-type, 4739 $\pm$ 417; $GFR\alpha3^{tlacZ/}$ ^{tlacZ}, 4133 $\pm$ 390; p = 0.34) in wild-type and mutant mice. Thus, in contrast to the effects of GDNF on enteric and parasympathetic neuroblasts (Enomoto et al., 2000; Young and Newgreen, 2001) and in contrast to a previous report on $GFR\alpha3^{-/-}$ mice (Andres et al., 2001), the proliferation rate of SCG sympathetic precursors in the mutant embryos were not statistically different than that observed in wild-type embryos. Taken together, these results indicate that ARTN appears to influence SCG development via its effect on cell migration and axonal projection but does not directly influence either survival or proliferation.

Neither ARTN nor GFRα3 Deficiency Cause Sensory Nervous System Deficits

GFRα3 is highly expressed in neurons of the peripheral sensory ganglia, such as the DRG, trigeminal, and glossopharyngeal ganglia (Figure 2) (Baloh et al., 1998a; Naveilhan et al., 1998; Widenfalk et al., 1998). Previous work has shown that nociceptive IB4$^+$ neurons in the DRG express Ret postnatally and that GDNF, NRTN, and ARTN promote their survival in vitro (Baudet et al., 2000; Molliver et al., 1997). The DRGs in adult $ARTN^{-/-}$ mice appeared of normal size and were morphologically normal under microscopic examination. To determine whether subpopulations of DRG neurons might be affected by ARTN deficiency, we examined IB4$^+$ and CGRP$^+$ neurons, but no deficits were observed (Figure 7A). To investigate whether the ARTN target population in the DRG, namely, GFRα3$^+$ neurons, was abnormal in the absence of ARTN, we examined wild-type and ARTN-deficient mice containing a single $GFR\alpha3^{tlacZ}$ allele. X-gal staining in these mice allowed for the examination of GFRα3$^+$ neurons, including their axonal projection patterns, in the presence or absence of ARTN. Surprisingly, we found that lack of ARTN did not affect the innervation pattern of the DRG GFRα3$^+$ neurons (Figures 7B and 7C).

Blood Vessel Smooth Muscle Cells Express ARTN

It is well established that sympathetic fibers follow blood vessels to reach their targets; however, the molecules and cell types involved in this phenomenon are unclear. The realization that ARTN is crucial for proper sympathetic innervation and that it is expressed around blood vessels suggests that it is an important guidance molecule for sympathetic axons. Thus, the identification of the cell type(s) in the blood vessels that express ARTN is of great interest. We performed double-label immunohistochemistry on sections through the superior mesenteric artery of $ARTN^{+/-}$ mice of various ages using antibodies to lacZ and to either anti-α-smooth muscle actin (a marker for smooth muscle cells) or vonWillebrand factor (a marker of endothelial cells). We found that lacZ staining in embryos overlapped with anti-smooth muscle actin antibody staining but not with vonWillebrand
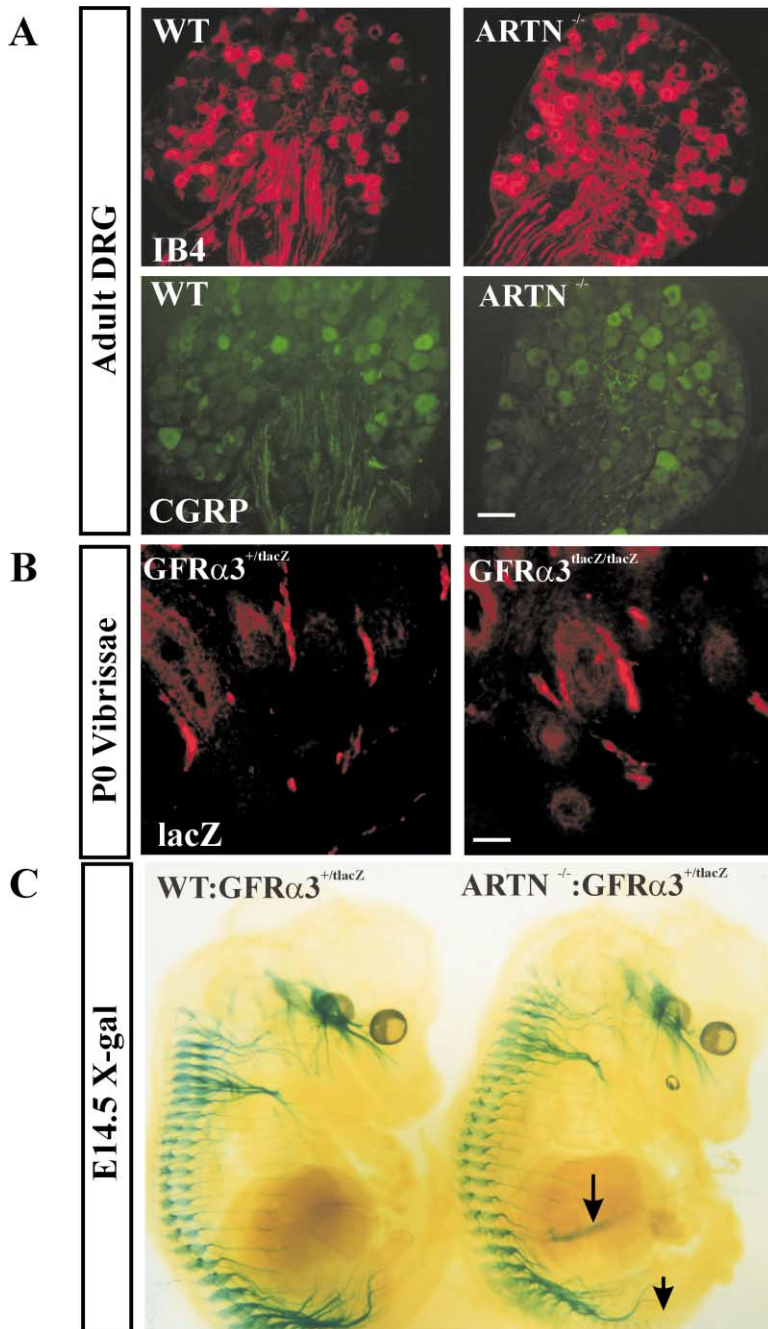
Figure 7. *ARTN*^{−/−} and *GFRα3*[tlacZ/tlacZ] Mice Do Not Have Deficits in DRG Sensory Neurons

(A) Adult DRG from wild-type and *ARTN*^{−/−} mice were stained with the lectin IB4 or anti-CGRP. No apparent differences in cell number were observed. (B) LacZ immunohistochemistry on P0 pups revealed that innervation of the vibrissae by GFRa3-expressing trigeminal ganglion fibers was similar in *GFRa3*[tlacZ/tlacZ] versus *Gfra3*[+/tlacZ] mice. (C) GFRa3-positive fibers from sensory ganglia were compared in *GFRa3*[+/tlacZ] mice either lacking ARTN or wild-type at the ARTN locus. Whole-mount X-gal staining of E14.5 embryos of both genotypes showed similar sensory neuron projection patterns. Scale bar, 100 mm in (A), 50 mm in (B). Arrows ([C], right panel) indicate lacZ staining corresponding to ARTN (not GFRa3) expression in the mesenteric artery and sclerotomes.

factor staining (Figure 8A). These results indicate that ARTN is synthesized in the smooth muscle cells of the blood vessel, a finding that is consistent with a previous suggestion that smooth muscle cells are important for the induction of sympathetic axonal outgrowth (Damon, 2001). ARTN expression was also detected in P6 gut vessels but was absent in adult gut (Figure 8A). Thus, ARTN is not expressed in the final target tissue (i.e., gut) after sympathetic innervation is established, a finding that is consistent with the idea that ARTN is unlikely to play a role in adulthood, and that ARTN and neurotrophins have different roles in forming and maintaining the sympathetic nervous system.

ARTN Is a Chemoattractant Specific for Sympathetic Nervous System

The analysis of ARTN-deficient mice, its expression pattern, and in vitro evidence (Enomoto et al., 2001) suggest that ARTN acts as a chemoattractant for sympathetic neurons. To address this issue further, we examined ARTN heterozygote E12 embryos to determine whether sympathetic axonal projections extended into regions of ARTN expression. Double-label staining using anti-TH to identify the sympathetic fibers and X-gal staining to detect ARTN expression was used to show that projections from the primordial SCG grow directly into a field of ARTN-expressing cells (Figure 8B). These results
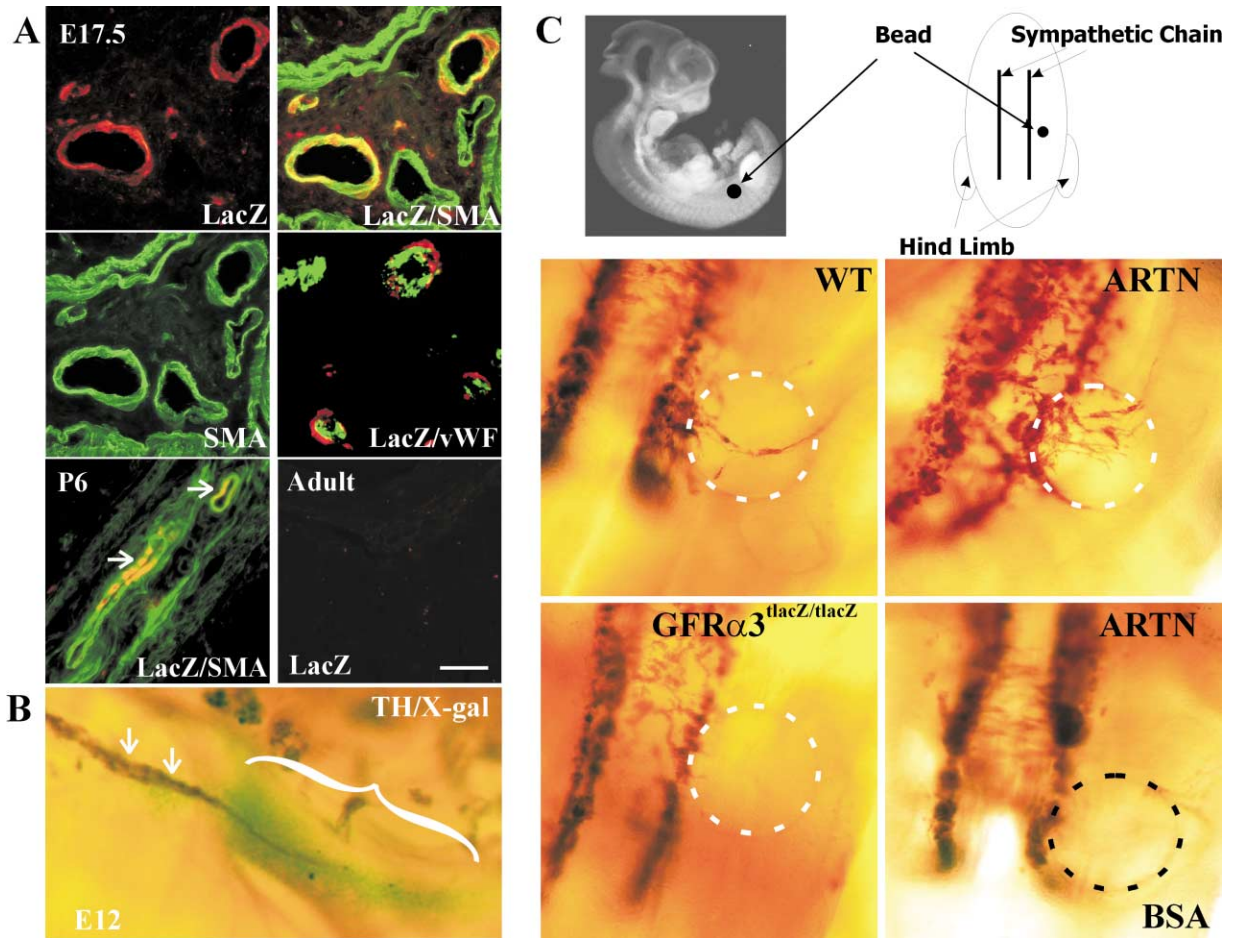
Figure 8. ARTN Is Expressed in Vascular Smooth Muscle Cells and Acts as a Chemoattractant for Sympathetic Neuroblasts and Axons

(A) Localization of ARTN expression using anti-lacZ immunohistochemical analysis of $ARTN^{+/-}$ mice. Double-label immunohistochemistry with anti-lacZ and anti-α-smooth muscle actin (SMA), a marker of smooth muscle cells, revealed that ARTN is expressed in vascular smooth muscle cells at E17.5. Similar analysis using anti-vonWillebrand factor (vWF) revealed no overlap, indicating ARTN is not expressed in endothelial cells. LacZ (ARTN) expression in SMA-positive cells was still observed in the gut wall at P6, but lacZ expression was not detected in adult gut.

(B) Double-label staining of E12 $ARTN^{+/-}$ embryos using whole-mount TH immunohistochemistry and X-gal staining revealed that TH-positive fibers emanating from the SCG (arrows) grow directly into areas expressing ARTN (bracket).

(C) ARTN influences sympathetic neuroblasts. An ARTN-soaked bead was placed in close proximity to the sympathetic chain in E11.5 embryos, the embryos were cultured for 24 hr, and whole-mount TH immunohistochemistry was performed. The ARTN-soaked bead induced neuronal migration and axonal outgrowth from sympathetic chain in wild-type and $ARTN^{-/-}$ mice. Note the dramatic effects of ectopic ARTN in $ARTN^{-/-}$ mice compared with that in wild-type mice. The ARTN-soaked bead failed to show any effect on the sympathetic chain in $GFR\alpha3^{tlacZ/tlacZ}$ mice. BSA-soaked bead (control) did not have any effect on sympathetic neuroblasts. Each experiment was performed from four to eight times with similar results. Scale bar, 50 μm in (A).

are consistent with a role for ARTN in guiding sympathetic axons. To test this hypothesis directly, the ability of ARTN to influence axonal growth was examined using whole-mount mouse embryo culture experiments (Martin and Cockroft, 1999). Since sympathetic neurons start extending their axons around E10.5–E11.5, we cultured E11.5 embryos in which acrylic beads incubated in ARTN or BSA were placed close to the sympathetic chain (Figure 8C). Twenty-four hours later, embryos were stained with either TH or neurofilament antibodies to examine the effects of the beads on axonal projections of the sympathetic (anti-TH) or other neuron populations (anti-neurofilament). In wild-type embryos, the ARTN-soaked beads induced axonal outgrowth from the sympathetic chain. However, when we put the bead

into the $ARTN^{-/-}$ embryo, a much more profound effect was observed. Robust neurite outgrowth directed toward the bead as well as many neurons migrating toward the ARTN-soaked bead were observed. No evidence of neurite outgrowth or cell migration was detected in embryos where BSA-soaked beads were used. Furthermore, sympathetic fibers did not respond when GDNF-soaked beads were implanted into these embryos (data not shown). Moreover, the ARTN-induced neuronal migration and axonal outgrowth was specific to the sympathetic nervous system, as whole-mount neurofilament immunostaining showed no fibers, other than those from the sympathetic chain, extending toward the ARTN-soaked bead. For example, sensory fibers from the DRG, which also express GFRα3 at this stage, did not appear

to be influenced by ectopic ARTN (data not shown). As a further control for the specificity of these effects and to examine ligand specificity in vivo, we placed ARTN-soaked beads into $GFR\alpha3^{tlacZ/tlacZ}$ mice. We found that ARTN had no effect on the sympathetic nervous system of $GFR\alpha3^{tlacZ/tlacZ}$ mice. These data indicate that ARTN acts as a guidance molecule that induces migration and axonal projection from sympathetic neurons through Ret:GFRα3 complexes.

Discussion

ARTN is the most recently identified member of the GFL neurotrophic factor family. It signals through the Ret/GFRα3 receptor complex and promotes the survival of a number of neuronal populations in vitro. To examine its physiological roles, we generated and characterized ARTN-deficient mice as well as GFRα3-deficient mice. Consistent with the in vivo preferential pairing of other GFL and GFRα receptors in mutant mice, the ARTN and GFRα3 mutants have identical phenotypes, including the variable penetrance of the SCG phenotype. Indeed, Ret mutant mice generated in our laboratory also display variability in the sympathetic defects with respect to position and size (Enomoto et al., 2001). In contrast, a previous report indicated that the SCG in all GFRα3 mutant mice was severely affected (Nishino et al., 1999). Although it is unclear why these phenotypic differences exist, it is presumably due to genetic background effects. Through the analysis of the ARTN and GFRα3 mice, we demonstrated that ARTN plays a crucial role in the development of the sympathetic nervous system. In the absence of ARTN-mediated signaling, numerous deficits in the entire sympathetic nervous system are apparent. ARTN is essential for the proper migration of sympathetic neuroblasts, and its absence results in defects throughout the sympathetic nervous system. Most dramatically, the failure to migrate properly results in the aberrant position of the SCG, which leads to ptosis due to the lack of sympathetic innervation to the superior tarsus muscle. The more severe effects observed for the SCG are likely due to the greater migration distance that these precursors must traverse; however, it could also be related to the different cellular origin of these cells. ARTN also plays an important role in stimulating axonal outgrowth from the sympathetic precursors. ARTN is expressed by vascular smooth muscle-like cells along the routes of sympathetic innervation, and ARTN- and GFRα3-deficient mice have dramatically abnormal projection patterns from all sympathetic ganglia. Consistent with these deficits in loss-of-function mutants, in vivo gain-of-function analysis demonstrated that ARTN acts as a guidance factor for the sympathetic nervous system in a GFRα3-dependent fashion.

In adult ARTN- and GFRα3-deficient mice with normal innervation of the superior tarsus muscle (i.e., without ptosis), the number of neurons in the SCG is normal. Furthermore, the level of proliferation and apoptosis in the SCG precursors is normal at all developmental periods examined. These data suggest that, despite the decreased number of total sympathetic neuroblasts in the vicinity of the dorsal aorta in E10.5 $GFR\alpha3^{tlacZ/tlacZ}$ embryos, normal numbers of SCG precursors must be present. Indeed, we found a less severe decrease in neuroblasts in the rostral portion, where the SCG precursors are predominantly localized. These rostral-caudal differences in sympathetic deficits are not unique to ARTN- and GFRα3-deficient mice. For example, mice lacking Phox2a have sympathetic defects only in the rostral ganglia, even though Phox2a is uniformly expressed throughout the sympathetic nervous system (Morin et al., 1997). On the other hand, ErbB3-deficient mice have deficits in sympathetic chain formation with no apparent defects in SCG precursors (Britsch et al., 1998). Furthermore, we have previously shown that Ret-deficient mice have a 30% decrease in SCG precursors; however, this is not due to a lack of ARTN-mediated signaling, as no deficits in SCG precursors are found in $ARTN^{-/-}$ mice. Indeed, earlier studies reported that GDNF-deficient mice have 20%–35% fewer SCG neurons at P0 (Moore et al., 1996; Sanchez et al., 1996), thus, it appears that GDNF may influence SCG precursors. In contrast, ARTN appears to be crucial for the migration of sympathetic chain precursors. Taken together, these results suggest that multiple GFLs contribute to the early development of the sympathetic ganglia.

Sympathetic nerves follow the vasculature to reach their final target tissues. This led to the suggestion that cells of the blood vessels produce guidance cues for sympathetic axons en route to their innervation targets. Once the axonal fibers reach their peripheral targets, sympathetic neuron survival is sustained by NGF. We have shown that ARTN is expressed along a number of blood vessels during the period of sympathetic innervation in a pattern consistent with a role in directing growth cone extension. For instance, ARTN expression in the mesenteric artery begins in the proximal regions of the vessel near the dorsal aorta and, as development proceeds, extends peripherally to distal segments of the vessel as it enters the gut. Double-label experiments demonstrated that ARTN is expressed in cells that express α-SMA (α-smooth muscle actin), a marker of smooth muscle and myofibroblast type cells, but not in endothelial cells. In addition, in the rat orbit, the sympathetic innervation of the tarsus and orbital muscles follows α-SMA$^+$ myofibroblast-like pathway cells (Smith et al., 1998). These α-SMA$^+$ myofibroblast-like cells also accompany the sympathetic hyperinnervation commonly observed in wound granulation tissue (Kishimoto et al., 1982). Thus, it appears that ARTN may be the neurotropic substance produced by α-SMA$^+$ cells of blood vessels that influences sympathetic neurons.

The sympathetic projections in ARTN- or GFRα3-deficient mice were shorter than normal and misdirected, indicating that ARTN-mediated signaling through Ret:GFRα3 complexes is necessary for proper innervation of target tissues. These deficits were observed as early as E11.5–E12.5, at a time when sympathetic precursors are just initiating axonal outgrowth, suggesting that Ret signaling is important for the early outgrowth pattern of axons. This abnormal initial outgrowth caused a delay in sympathetic innervation; however, compensatory mechanisms must exist, as most tissues eventually become at least partially innervated. The role of ARTN as a guidance factor for sympathetic axons is supported by gain-of-function experiments in which ARTN-impregnated beads were implanted in mouse embryos. These

experiments revealed that axons emanating from sympathetic precursors grew toward the ARTN-soaked beads in a directed fashion; however, sympathetic fibers of embryos lacking GFRα3 did not grow toward the ARTN source. Thus, ARTN fulfills three important criteria of a neuronal guidance cue: (1) it is expressed at the correct time and place to influence sympathetic axons, (2) loss-of-function mutations lead to aberrant sympathetic innervation, and (3) sympathetic axons grow toward an ectopic source of ARTN.

Although ARTN is capable of promoting survival of multiple neuronal populations in vitro, its physiologic role as a sympathetic neuron survival factor in vivo is unlikely. The rate of apoptosis in developing sympathetic ganglia was not uniformly increased in $ARTN^{-/-}$ embryos. Apoptosis in the SCG is elevated only when the ganglion is caudally positioned with the accompanying deficits in target innervation. Those SCG in only a slightly abnormal position do not show increased levels of apoptosis or decreased numbers of sympathetic neurons. In contrast, SCG that do not properly innervate their targets due to their caudal location have severely decreased cell numbers. From this analysis, it appears that the SCG neuronal loss observed in ARTN-deficient mice is secondary to its role as a guidance factor. Without ARTN, the sympathetic neuroblasts fail to migrate properly, and the sympathetic axons fail to innervate their targets. Thus, the SCG neurons fail to secure the target derived neurotrophic support (NGF) that is essential for their survival. This is a continuing theme in GFL biology, where it is becoming clear that cell migration and axonal outgrowth are their primary roles in development. For example, enteric neurons in GDNF-deficient mice fail to migrate along the gastrointestinal tract, the ureteric bud fails to move into the metanephrogenic blastema in the developing kidney, and parasympathetic neurons fail to migrate and form the sphenopalatine and otic ganglia (Moore et al., 1996; Pichel et al., 1996; Sanchez et al., 1996; Schuchardt et al., 1996; Enomoto et al., 2000). In addition, GDNF stimulates migration of kidney cells in vitro (Tang et al., 1998). ARTN appears unique as a "neurotrophic" factor because it acts as a guidance factor without influencing directly neuronal survival in vivo; i.e., its physiologic role is primarily neurotropic rather than neurotrophic. Its function as an intermediate guidance cue is also unique because other such cues, like the netrins, are both attractive and repulsive (Song and Poo, 1999). In contrast, ARTN always acts as an attractant, and therefore, its ability to guide axons is due to its continuously changing expression pattern that leads axons toward the final peripheral target.

The importance of the neurotrophins in the development of the sympathetic nervous system is well documented. NGF and NT-3 secured from the innervated targets are crucial for sympathetic neuronal survival. Indeed, analysis of mice lacking either NT-3 or NGF demonstrated that sympathetic neuronal death temporally coincided in both mutants and indicated that these neurotrophins support newly generated sympathetic neurons but do not influence sympathetic precursors (Francis, et al., 1999). The effects of both NT-3 and NGF are mediated through TrkA, as TrkC-deficient mice do not have reduced numbers of SCG neurons (Tessarollo

et al., 1997). In addition, neurotrophins are required for proper innervation of distal targets but not for initial neurite outgrowth. This has been documented using both TrkA-deficient (Fagan et al., 1996) and NT3-deficient mice, in which sympathetic fibers approach but fail to invade their targets (ElShamy et al., 1996). It is now apparent that ARTN plays an early role in stimulating axonal outgrowth as a paracrine factor and in attracting axons to intermediate targets such as blood vessels to facilitate innervation of the final target. Subsequently, NGF and NT-3, acting as target-derived factors, become crucial for supporting the sympathetic neurons and promoting axonal arborization within the target tissue (Hoyle et al., 1993). Changes in trophic factor dependence also occur in the parasympathetic nervous system. Neuronal precursors of the sphenopalatine and otic ganglia, for example, depend on locally expressed GDNF to stimulate proliferation and migration during embryonic development, but neurons of these ganglia are supported in adulthood by NRTN acquired from their innervation targets. Thus, in the case of the parasympathetic nervous system, the supporting trophic factors for developing and mature neurons are both GFLs. The situation is somewhat different in sympathetic neurons, as it involves a change from GFL-mediated Ret signaling to NGF-stimulated TrkA signaling. In the DRG sensory ganglia, trophic factor class switching also occurs, but in this case, early postnatal sensory neurons switch from neurotrophin to GFL-mediated signaling (Molliver et al., 1997). Thus, there are now multiple examples where GFL and neurotrophin signaling are both required for proper development and maintenance of specific neuronal populations. The physiologic purpose of changing between Ret and Trk signaling will require further dissection of the signaling pathways emanating from these receptors. Future studies in this regard are likely to yield new insights into how neurotrophic factors influence neuronal function.

Experimental Procedures

Generation of ARTN and GFRα3-Deficient Mice

BAC clones (strain 129/SvJ) containing either the murine *ARTN* or *GFRα3* genes were obtained from Genome Systems. To construct the ARTN targeting vector, which contains a 4.1 kb 5′ fragment and a 1.7 kb 3′ fragment, the lacZ gene was cloned upstream of the Tn5 neo cassette flanked by loxP sites, and this fragment was inserted into the first coding exon of the *ARTN* gene by bacterial homologous recombination (Zhang et al., 1998). This deletes 808 nt that encompass the initiator Met and 127 downstream residues. To construct the *GFRα3* targeting vector, which contains a 6 kb 5′ fragment and a 2.2 kb 3′ fragment, the *tau-lacZ* gene (Callahan and Thomas, 1994) was cloned upstream of the Tn5 neo cassette flanked by loxP sites, and this fragment was inserted into the first coding exon of the *GFRα3* gene by bacterial recombination. This deletes 92 nt that includes the initiator Met and 23 downstream residues. The linearized targeting constructs in which lacZ reporters were "knocked in" to *ARTN* or *GFRα3* genes were electroporated into the 129/SvJ embryonic stem (ES) cell line RW4, and homologous recombinants were identified by Southern blot hybridization. Properly targeted ES cells clones were injected into C57BL/6 blastocysts to generate chimeric mice that successfully achieved germline transmission of the targeted allele (either ARTN or GFRα3). Both ARTN and GFRα3 heterozygous animals were further crossed with β-actin Cre transgenic mice (Lewandoski et al., 1997) to remove the Tn5 neo cassette and prevent potential transcriptional interference of the lacZ reporter genes and to generate thereby the knock-in alleles referred

to as *ARTN*⁻ and *GFRα3^tlacZ*. Mice heterozygous for the mutant *ARTN* or *GFRα3* alleles were mated to obtain ARTN- and GFRα3-deficient animals. Analyses were performed on mice with a hybrid 129/SvJ:C57BL/6 background. The genotypes of *ARTN*⁻/⁻ mice were determined by Southern blotting or PCR using a three primer system (5′-TCGAGAGACTGGAGTGGAAGGAGGAA, 5′-TTGGCATTTCCCC TTTCATATTCTGA, and 5′-ACCAGGCAAAGCGCCATTCGC). The genotypes of *GFRα3^tlacZ* mice were determined by Southern blotting or PCR using a three primer system (5′-CGGCGCCCAGCGCAGG CAGAGCGCTGT, 5′-GGTCCATGTCACCCTCCTGGTCTTGCA, and 5′-ACCCTACAGCCCAGAGGGTTTCTGAAT).

RT-PCR was performed using RNA from whole P0 homozygous pups as template to confirm that *ARTN^tlacZ/tlacZ* and *GFRα3^tlacZ/tlacZ* mice were null for ARTN and GFRα3, respectively. ARTN primers: 5′-TAC TGCATTGTCCCACTGCCTCC and 5′-TCGCAGGGTTCTTTCGCTG CACA; GFRα3 primers: 5′-CGGCGCCCAGCGCAGGCAGAGCGC TGT and 5′-GTCTGCAGACATGGCAGACTCCTCTAA. GAPDH was used as an internal control to insure equal input RNA template.

Histological Analysis
Embryos were obtained from timed pregnancies and were staged according to their somite numbers and overall appearance. Tissues were prepared, stained, and sectioned essentially as described (Enomoto et al., 1998). For adult SCG and prevertebral ganglia analysis, adult head and body were treated by 10% EDTA for 3–4 weeks for decalcification. After decalcification, tissues were embedded in paraffin, then sectioned and stained as above. Immunohistochemistry was performed on either frozen or paraffin-embedded sections as described (Enomoto et al., 1998) using the following antibodies: 2H3 anti-neurofilament (Developmental Studies Hybridoma Bank [DSHB]), p75 (Chemicon), β-galactosidase (Biogenesis), Ret (IBL, R&D), Smooth muscle actin (DAKO), vonWillebrand factor (DAKO), Phox2a and 2b (gift from J.-F. Brunet, INSERM, Marseille), BrdU (Roche), TH (Chemicon), active-caspase 3 (Cell Signaling), CGRP (INCSTAR), biotinylated-rabbit, goat, mouse, sheep minimal cross reactive secondary antibodies (Jackson), Alexa488-rabbit, mouse minimal cross reactive secondary antibodies (Molecular Probes). When signal amplification of the immunohistochemistry was necessary, the TSA and TSA-plus systems (Perkin-Elmer) were used. X-gal staining was performed essentially as described (Francis et al., 1999). TUNEL staining was performed as described (Enomoto et al., 2001). IB4 staining was done as described (Molliver et al., 1997). Whole-mount immunohistochemistry for TH and acetylcholinesterase was performed as described (Enomoto et al., 2001; Heuckeroth et al., 1999).

Quantitative analysis of the enteric nervous system was performed as previously described (Heuckeroth et al., 1999). Submucosal neuron counts were performed on acetylcholinesterase-stained tissue. Myenteric neuron counts were performed on cuprolinic blue-stained tissue. Cells were counted at 200× using a 2.5 × 10⁻³ cm² counting grid. Cells from each animal were counted in 20 random fields for both the small bowel and colon. The average number of cells per grid was determined, and the data were entered into SigmaPlot and analyzed using SigmaStat statistical software. TH-positive fiber counts in the myenteric plexus of the small bowel were determined by counting the number of fibers which passed through a 0.5 mm line of a 2.5 × 10⁻³ cm² counting grid which was placed perpendicular to the TH-positive fibers at 200×. Fibers for each animal were counted in 20 random fields, and the data were entered into SigmaPlot and analyzed using SigmaStat statistical software.

To quantify the number of proliferating sympathoblasts in embryonic SCG, BrdU (Sigma) was injected intraperitoneally into pregnant mice (6 mg/mice) 1 hr prior to harvesting the embryos. Embryos (wild-type and *GFRα3^tlacZ/tlacZ*, n = 5) were fixed in 4% paraformaldehyde, embedded in paraffin, and consecutive 5 μm sections were cut. For the E12.5 wild-type and GFRa3 embryos, the entire ganglion was counted. For this analysis, every third section was incubated with Phox2b antibody (1:4000) after antigen-retrieval (1 mM EDTA for 30 min at 100°C) followed by incubation with biotinylated rabbit secondary antibody and avidin-biotin Cy3. The sections were then incubated with mouse BrdU antibody (1:200) and labeled with Alexa488 conjugated secondary mouse antibody. The double positive (Phox2b⁺/BrdU⁺) cells were counted. For calculation of percent-

ages of proliferating neurons from representative sections of E11.5 and E14.5 embryos, three sections (from three embryos of each genotype) were stained as above, and all Phox2b⁺ and Phox2b/BrdU-double positive cells were counted.

To determine the total number of neurons per ganglia, consecutive 5 μm sections of paraffin-embedded tissues were cut and stained with thionin. Neurons with visible nucleoli were counted on every third section, and the total counts were tripled to calculate the total number of neurons (Enomoto et al., 1998; Heuckeroth et al., 1999). All statistical analysis was performed using the Student's t test.

Quantitative analysis of sympathetic precursors was performed as previously described (Britsch et al., 1998). Briefly, E10.5 embryos were staged according to their somite numbers (30–35 somites) and overall appearance. They were fixed in 4% paraformaldehyde for 2 hr, washed in PBS, and embedded in OCT (Sacra) after cryoprotection in 30% sucrose/PBS. Consecutive frozen sections (12 μm) of the entire forelimb region were prepared. Every third section from three embryos of each genotype was stained with Phox2b antibody, and the Phox2b⁺ cells surrounding the dorsal aorta were counted. The average number of Phox2b⁺ cells per section was compared between wild-type and *GFRα3^tlacZ/tlacZ* embryos using SigmaStat software.

Whole-Mount Embryo Culture
Embryos were cultured essentially as described (Martin and Cockroft, 1999). ARTN-, GDNF-, and BSA-impregnated beads were prepared as described (Tang et al., 1998). Heparin-acrylic beads (Sigma) were washed in PBS and incubated with 10 ng/μl recombinant ARTN, GDNF, or BSA (Sigma) for 1 hr. Beads were washed in PBS, and a single bead was inserted into E11.5 embryos. After culturing for 24 hr, embryos were fixed in 4% paraformaldehyde for 16 hr, washed in PBS, and stained using TH and 2H3 neurofilament antibodies.

References

Albers, K.M., Perrone, T.N., Goodness, T.P., Jones, M.E., Green, M.A., and Davis, B.M. (1996). Cutaneous overexpression of NT-3 increases sensory and sympathetic neuron number and enhances touch dome and hair follicle innervation. J. Cell Biol. *134*, 487–497.

Anderson, D.J., Groves, A., Lo, L., Ma, Q., Rao, M., Shah, N.M., and Sommer, L. (1997). Cell lineage determination and the control of neuronal identity in the neural crest. Cold Spring Harb. Symp. Quant. Biol. *62*, 493–504.

Andres, R., Forgie, A., Wyatt, S., Chen, Q., de Sauvage, F.J., and Davies, A.M. (2001). Multiple effects of artemin on sympathetic neurone generation, survival and growth. Development *128*, 3685–3695.

Baloh, R.H., Gorodinsky, A., Golden, J.P., Tansey, M.G., Keck, C.L., Popescu, N.C., Johnson, E.M., Jr., and Milbrandt, J. (1998a). GFRa3 is an orphan member of the GDNF/neurturin/persephin receptor family. Proc. Natl. Acad. Sci. USA *95*, 5801–5806.

Baloh, R.H., Tansey, M.G., Lampe, P.A., Fahrner, T.J., Enomoto, H., Simburger, K., Leitner, M.L., Araki, T., Johnson, E.M.J., and Milbrandt, J. (1998b). Artemin, a novel member of the GDNF ligand family supports peripheral and central neurons and signals through the GFRa3-RET receptor complex. Neuron *21*, 1291–1302.

Baloh, R.H., Enomoto, H., Johnson, E.M., Jr., and Milbrandt, J.

(2000). The GDNF family ligands and receptors - implications for neural development. Curr. Opin. Neurobiol. *10*, 103–110.

Barbacid, M. (1994). The Trk family of neurotrophin receptors. J. Neurobiol. *25*, 1386–1403.

Baudet, C., Mikaels, A., Westphal, H., Johansen, J., Johansen, T.E., and Ernfors, P. (2000). Positive and negative interactions of GDNF, NTN and ART in developing sensory neuron subpopulations, and their collaboration with neurotrophins. Development *127*, 4335–4344.

Bibel, M., and Barde, Y.A. (2000). Neurotrophins: key regulators of cell fate and cell shape in the vertebrate nervous system. Genes Dev. *14*, 2919–2937.

Britsch, S., Li, L., Kirchhoff, S., Theuring, F., Brinkmann, V., Birchmeiner, C., and Riethmacher, D. (1998). The ErbB2 and ErbB3 receptors and their ligand, neuregulin-1, are essential for development of the sympathetic nervous system. Genes Dev. *12*, 1825–1836.

Callahan, C.A., and Thomas, J.B. (1994). Tau-beta-galactosidase, an axon-targeted fusion protein. Proc. Natl. Acad. Sci. USA *91*, 5972–5976.

Chalazonitis, A., Rothman, T.P., Chen, J., and Gershon, M.D. (1998). Age-dependent differences in the effects of GDNF and NT-3 on the development of neurons and glia from neural crest-derived precursors immunoselected from the fetal rat gut: expression of GFRalpha-1 in vitro and in vivo. Dev. Biol. *204*, 385–406.

Christiansen, J.H., Coles, E.G., and Wilkinson, D.G. (2000). Molecular control of neural crest formation, migration and differentiation. Curr. Opin. Cell Biol. *12*, 719–724.

Costa, M., and Furness, J.B. (1984). Somatostatin is present in a subpopulation of noradrenergic nerve fibres supplying the intestine. Neuroscience *13*, 911–919.

Damon, D.H. (2001). NGF-independent survival of postganglionic sympathetic neurons in neuronal-vascular smooth muscle cocultures. Am. J. Physiol. Heart Circ. Physiol. *280*, H1722–H1728.

Durbec, P.L., Larsson-Blomberg, L.B., Schuchardt, A., Costantini, F., and Pachnis, V. (1996). Common origin and developmental dependence on c-ret of subsets of enteric and sympathetic neuroblasts. Development *122*, 349–358.

ElShamy, W.M., Linnarsson, S., Lee, K.F., Jaenisch, R., and Ernfors, P. (1996). Prenatal and postnatal requirements of NT-3 for sympathetic neuroblast survival and innervation of specific targets. Development *122*, 491–500.

Enomoto, H., Araki, T., Jackman, A., Heuckeroth, R.O., Snider, W.D., Johnson, E.M., Jr., and Milbrandt, J. (1998). GFR a1-deficient mice have deficits in the enteric nervous system and kidneys. Neuron *21*, 317–324.

Enomoto, H., Heuckeroth, R.O., Golden, J.P., Johnson, E.M., and Milbrandt, J. (2000). Development of cranial parasympathetic ganglia requires sequential actions of GDNF and neurturin. Development *127*, 4877–4889.

Enomoto, H., Crawford, P.A., Gorodinsky, A., Heuckeroth, R.O., Johnson, E.M., Jr., and Milbrandt, J. (2001). RET signaling is essential for migration, axonal growth and axon guidance of developing sympathetic neurons. Development *128*, 3963–3974.

Fagan, A.M., Zhang, H., Landis, S., Smeyne, R.J., Silos-Santiago, I., and Barbacid, M. (1996). TrkA, but not TrkC, receptors are essential for survival of sympathetic neurons in vivo. J. Neurosci. *16*, 6208–6218.

Fernholm, M. (1971). On the development of the sympathetic chain and the adrenal medulla in the mouse. Z. Anat. Entwicklungsgesch. *133*, 305–317.

Francis, N., Farinas, I., Brennan, C., Rivas-Plata, K., Backus, C., Reichardt, L., and Landis, S. (1999). NT-3, like NGF, is required for survival of sympathetic neurons, but not their precursors. Dev. Biol. *210*, 411–427.

Garcia-Castro, M., and Bronner-Fraser, M. (1999). Induction and differentiation of the neural crest. Curr. Opin. Cell Biol. *11*, 695–698.

Goldstein, R.S., and Kalcheim, C. (1991). Normal segmentation and size of the primary sympathetic ganglia depend upon the alternation of rostrocaudal properties of the somites. Development *112*, 327–334.

Guillemot, F., Lo, L.-C., Johnson, J.E., Auerbach, A., Anderson, D.J., and Joyner, A.L. (1993). Mammalian achaete-scute Homolog 1 is required for the early development of olfactory and autonomic neurons. Cell *75*, 463–476.

Hearn, C.J., Murphy, M., and Newgreen, D. (1998). GDNF and ET-3 differentially modulate the numbers of avian enteric neural crest cells and enteric neurons in vitro. Dev. Biol. *197*, 93–105.

Heuckeroth, R.O., Lampe, P.A., Johnson, E.M., and Milbrandt, J. (1998). Neurturin and GDNF promote proliferation and survival of enteric neuron and glial progenitors in vitro. Dev. Biol. *200*, 116–129.

Heuckeroth, R.O., Enomoto, H., Grider, J.R., Golden, J.P., Hanke, J.A., Jackman, A., Molliver, D.C., Bardgett, M.E., Snider, W.D., Johnson, E.M., Jr., and Milbrandt, J. (1999). Gene targeting reveals a critical role for neurturin in the development and maintenance of enteric, sensory, and parasympathetic neurons. Neuron *22*, 253–263.

Hirsch, M.R., Tiveron, M.C., Guillemot, F., Brunet, J.F., and Goridis, C. (1998). Control of noradrenergic differentiation and Phox2a expression by MASH1 in the central and peripheral nervous system. Development *125*, 599–608.

Hoyle, G.W., Mercer, E.H., Palmiter, R.D., and Brinster, R.L. (1993). Expression of NGF in sympathetic neurons leads to excessive axon outgrowth from ganglia but decreased terminal innervation within tissues. Neuron *10*, 1019–1034.

Huang, E.J., and Reichardt, L.F. (2001). Neurotrophins: roles in neuronal development and function. Annu. Rev. Neurosci. *24*, 677–736.

Kandel, E., Schwartz, J., and Jessell, T. (2000). Principles of Neural Science, Fourth edition (New York: McGraw Hill).

Kishimoto, S., Maruo, M., Ohse, C., Yasuno, H., Kimura, H., Nagai, T., and Maeda, T. (1982). The regeneration of the sympathetic catecholaminergic nerve fibers in the process of burn wound healing in guinea pigs. J. Invest. Dermatol. *79*, 141–146.

Kotzbauer, P.T., Lampe, P.A., Heuckeroth, R.O., Golden, J.P., Creedon, D.J., Johnson, E.M., and Milbrandt, J.D. (1996). Neurturin, a relative of glial-cell-line-derived neurotrophic factor. Nature *384*, 467–470.

Krull, C.E. (2001). Segmental organization of neural crest migration. Mech. Dev. *105*, 37–45.

LeDouarin, N.M. (1986). Cell line segregation during peripheral nervous system ontogeny. Science *231*, 1515–1522.

Lewandoski, M., Wassarman, K.M., and Martin, G.R. (1997). Zp3-cre, a transgenic mouse line for the activation or inactivation of loxP-flanked target genes specifically in the female germ line. Curr. Biol. *7*, 148–151.

Lin, L.-F.H., Doherty, D.H., Lile, J.D., Bektesh, S., and Collins, F. (1993). GDNF: A glial cell line-derived neurotrophic factor for midbrain dopaminergic neurons. Science *260*, 1130–1132.

Martin, P., and Cockroft, D.L. (1999). Culture of postimplantation mouse embryos. Methods Mol. Biol. *97*, 7–22.

Milbrandt, J., de Sauvage, F.J., Fahrner, T.J., Baloh, R.H., Leitner, M.L., Tansey, M.G., Lampe, P.A., Heuckeroth, R.O., Kotzbauer, P.T., Simburger, K.S., et al. (1998). Persephin, a novel neurotrophic factor related to GDNF and neurturin. Neuron *20*, 245–253.

Molliver, D.C., Wright, D.E., Leitner, M.L., Parsadanian, A.S., Doster, K., Wen, D., Yan, Q., and Snider, W.D. (1997). IB4-binding DRG neurons switch from NGF to GDNF dependence in early postnatal life. Neuron *19*, 849–861.

Moore, M.W., Klein, R.D., Farinas, I., Sauer, H., Armanini, M., Phillips, H., Reichart, L.F., Ryan, A.M., Carver-Moore, K., and Rosenthal, A. (1996). Renal and neuronal abnormalities in mice lacking GDNF. Nature *382*, 76–79.

Morin, X., Cremer, H., Hirsch, M.R., Kapur, R.P., Goridis, C., and Brunet, J.F. (1997). Defects in sensory and autonomic ganglia and absence of locus coeruleus in mice deficient for the homeobox gene Phox2a. Neuron *18*, 411–423.

Naveilhan, P., Baudet, C., Mikaels, A., Shen, L., Westphal, H., and Ernfors, P. (1998). Expression and regulation of GFRalpha3, a glial

cell line-derived neurotrophic factor family receptor. Proc. Natl. Acad. Sci. USA *95*, 1295–1300.

Nishino, J., Mochida, K., Ohfuji, Y., Shimazaki, T., Meno, C., Ohishi, S., Matsuda, Y., Fujii, H., Saijoh, Y., and Hamada, H. (1999). GFR alpha3, a component of the artemin receptor, is required for migration and survival of the superior cervical ganglion. Neuron *23*, 725–736.

Patel, T.D., Jackman, A., Rice, F.L., Kucera, J., and Snider, W.D. (2000). Development of sensory neurons in the absence of NGF/TrkA signaling in vivo. Neuron *25*, 345–357.

Pattyn, A., Morin, X., Cremer, H., Goridis, C., and Brunet, J.F. (1999). The homeobox gene Phox2b is essential for the development of autonomic neural crest derivatives. Nature *399*, 366–370.

Pichel, J.G., Shen, L., Hui, S.Z., Granholm, A.-C., Drago, J., Grinberg, A., Lee, E.J., Huang, S.P., Saarma, M., Hoffer, B.J., et al. (1996). Defects in enteric innervation and kidney development in mice lacking GDNF. Nature *382*, 73–76.

Rubin, E. (1985). Development of the rat superior cervical ganglion: ganglion cell maturation. J. Neurosci. *5*, 673–684.

Saarma, M., and Sariola, H. (1999). Other neurotrophic factors: glial cell line-derived neurotrophic factor (GDNF). Microsc. Res. Tech. *45*, 292–302.

Sanchez, M.P., Silos-Santiago, I., Frisen, J., He, B., Lira, S.A., and Barbacid, M. (1996). Renal agenesis and the absence of enteric neurons in mice lacking GDNF. Nature *382*, 70–73.

Schmidt, R., Dorsey, D., Selznick, L., DiStefano, P., Carroll, S., Beaudet, L., and Roth, K. (1998). Neurotrophin sensitivity of prevertebral and paravertebral rat sympathetic autonomic ganglia. J. Neuropathol. Exp. Neurol. *57*, 158–167.

Schneider, C., Wicht, H., Enderich, J., Wegner, M., and Rohrer, H. (1999). Bone morphogenetic proteins are required in vivo for the generation of sympathetic neurons. Neuron *24*, 861–870.

Schuchardt, A., D'Agati, V., Pachnis, V., and Costantini, F. (1996). Renal agenesis and hypodysplasia in ret-k-mutant mice result from defects in ureteric bud development. Development *122*, 1919–1929.

Smith, P.G., Fan, Q., Zhang, R., and Warn, J.D. (1998). Cellular terrain surrounding sympathetic nerve pathways in the rat orbit: comparisons of orbital connective tissue and smooth muscle cell phenotypes. J. Comp. Neurol. *400*, 529–543.

Snider, W.D., and Wright, D.E. (1996). Neurotrophins cause a new sensation. Neuron *16*, 229–232.

Song, H.J., and Poo, M.M. (1999). Signal transduction underlying growth cone guidance by diffusible factors. Curr. Opin. Neurobiol. *9*, 355–363.

Tang, M.J., Worley, D., Sanicola, M., and Dressler, G.R. (1998). The RET-glial cell-derived neurotrophic factor (GDNF) pathway stimulates migration and chemoattraction of epithelial cells. J. Cell Biol. *142*, 1337–1345.

Taraviras, S., Marcos-Gutierrez, C.V., Durbec, P., Jani, H., Grigoriou, M., Sukumaran, M., Wang, L.C., Hynes, M., Raisman, G., and Pachnis, V. (1999). Signalling by the RET receptor tyrosine kinase and its role in the development of the mammalian enteric nervous system. Development *126*, 2785–2797.

Tessarollo, L., Tsoulfas, P., Donovan, M., Palko, M., Blair-Flynn, J., Hempstead, B., and Parada, L. (1997). Targeted deletion of all isoforms of the trkC gene suggests the use of alternate receptors by its ligand neurotrophin-3 in neuronal development and implicates trkC in normal cardiogenesis. Proc. Natl. Acad. Sci. USA *94*, 14776–14781.

Widenfalk, J., Tomac, A., Lindqvist, E., Hoffer, B., and Olson, L. (1998). GFRalph3, a protein related to GFRa1, is expressed in developing peripheral neurons and ensheathing cells. Eur. J. Neurosci. *10*, 1508–1517.

Young, H.M., and Newgreen, D. (2001). Enteric neural crest-derived cells: origin, identification, migration, and differentiation. Anat. Rec. *262*, 1–15.

Zhang, Y., Buchholz, F., Muyrers, J.P., and Stewart, A.F. (1998). A new logic for DNA engineering using recombination in Escherichia coli. Nat. Genet. *20*, 123–128.